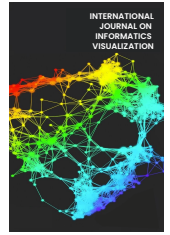




INTERNATIONAL JOURNAL ON INFORMATICS VISUALIZATION

journal homepage : www.joiv.org/index.php/joiv



Optimization of General Threshold Value for Pre-processing in Plasmodium Parasites Detection

Hanung Adi Nugroho ^{a,*}, Rizki Nurfauzi ^a

^a Department of Electrical and Information Engineering, Universitas Gadjah Mada, Depok, Sleman, 55281, Indonesia

Corresponding author: *adinugroho@ugm.ac.id

Abstract— The high mortality rate of malaria makes it a severe disease that spreads throughout all-region by infected female *Anopheles* mosquitoes, especially in tropical countries. Accurate early malaria detection is one of the ways to reduce the mortality rate. Microscopy-based malaria examinations are still considered the gold standard. Due to numerous large malaria patients with limited parasitologists, an automated detection system is needed as a second opinion to assist parasitologists. This study proposed an optimization method for finding an optimal global threshold value for pre-processing parasite detection. There were three stages of the proposed method. The first is to pre-process digital microscopic images using color channel selection, contrast stretching, and morphological operation. The second is to find the global threshold value using multiple modified Otsu's. The third is to determine the optimum global threshold value. In the last stage, predicted threshold values are generated using a pattern recognition approach to determine the optimum global threshold value. The proposed method evaluated 468 microscopic images captured from hundreds of thin smear blood slides. The slides are provided by the Department of Parasitology-UGM and the Eijkman Institute for Molecular Biology. The set image contains 691 malaria parasites in all types and life stages of malaria parasites. The proposed method obtained a sensitivity of 99.6 % and the smallest FPs number compared to without the optimization. It indicates that the proposed method has the potential to be implemented in the initial stages of the malaria detection system.

Keywords— Detection; Malaria; plasmodium; parasite; global thresholding.

Manuscript received 17 Oct. 2022; revised 21 Feb. 2023; accepted 25 Apr. 2023. Date of publication 31 Dec. 2023.
International Journal on Informatics Visualization is licensed under a Creative Commons Attribution-Share Alike 4.0 International License.



I. INTRODUCTION

The word “malaria” is derived from the Italian word *mal'aria* or “bad air” in English [1]. The World Health Organization (WHO) report shows that malaria is a severe public health problem. It spread to more than 90 countries in 2017; the number of dead people was estimated at 435,000 [2]. Children aged less than five years are the most vulnerable infected by malaria. In 2017, they accounted for up to 61% (266,000) of all malaria deaths worldwide. In the same year, the WHO in Africa Region record showed that the region became home to the highest number of malaria deaths worldwide [2]. In 2012, the Ministry of Health of Indonesia reported that there were 417,819 cases of malaria. In 2016, malaria cases decreased by about 218,450 cases. This fact indicates that Indonesia has made progress in eradicating malaria. However, malaria cases are still relatively high [3]. The characteristics of each type and life stage of malaria parasites can be seen in Figure 1.

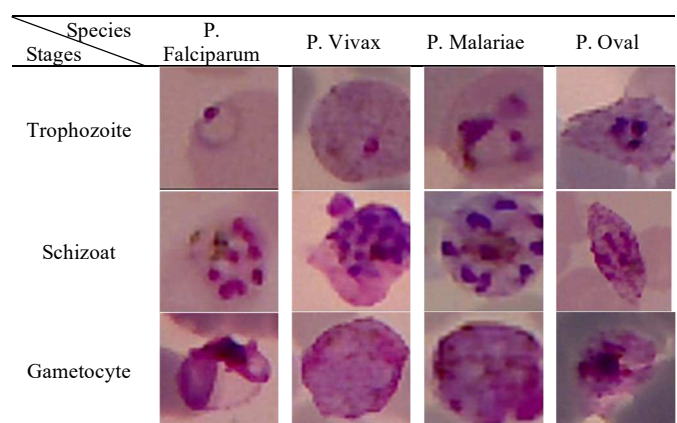


Fig. 1 Four different malaria parasite species and their three-stage life cycle [4].

An expert slide reader called parasitologist visually inspects blood slides for detecting the malaria parasites [5], [6]. This laborious and accurate laboratory diagnosis is essential for diagnosing and treating malaria properly.

However, since hundreds of millions of slides are examined every year around the world, error-prone processes or false-negative potential occur, causing severe consequences [7]. There is no standard for conducting microscopic diagnosing for malaria. It depends mostly on the parasitologist's or microscopist's expertise and experience [8], [9]. Several studies show that manual microscopy checks are not reliable screening methods since they are administered by less-experienced people, especially in rural areas where malaria is prevalent [9]–[12]. An automated system aims to carry out this task without human intervention and deliver an objective, reliable, and efficient system.

Microscopic slides utilized in malaria detection can be prepared in two different slides: thick and thin blood smears.

The advantages and disadvantages of each slide's use are clearly explained [9], [13], [14]. However, using a thin blood smear allows malaria experts to recognize a parasite's species and life stages. Therefore, the data utilized in this study were thin smear.

There is a multi-part problem of diagnosing malaria by computer vision. The parts are image acquisition, pre-processing, segmentation (object localization), and classification. However, when the system is demanded to be fully automated, several functions such as positioning microscope slides, reliable focusing, and shooting must also be automated [9]. Hence, several possible steps exist in designing computer-aided malaria detection (CAD), as shown in Figure 2.

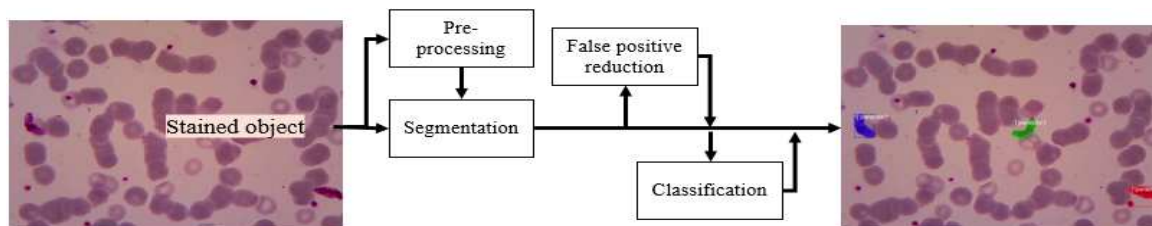


Fig. 2 Block diagram of possible ways in parasite segmentation

Pre-processing is the primary step of the general malaria CAD. The system for further analysis should detect all parasites. The overlooked parasites are impossible to recover in further steps. However, not many studies are focused on this step. In overcoming the limitation, the study's attention is on the pre-processing step. Therefore, this study aims to achieve higher sensitivity in detecting parasite candidates than the previously published studies. Several previous studies have been reviewed to support the achievement of the goals. The studies are listed below.

There are many recognized staining methods supported by [15]. However, Giemsa is the most popular and effective cost stain for the staining method [16]. The method only highlights parasites, white blood cells (WBC), platelets, and artifacts. Different filter methods can be applied to reduce the illumination effect obtained from both camera and microscope light. Human factors, inappropriate blood slides preparation due to non-standard, and the non-homogeneous staining concentration may also evoke luminance noise.

There are many developed techniques to overcome impulse noise, including mean filtering [17], [18], median filtering [19], Geometric mean filtering [20], [21], Gaussian low-pass filtering [22], Gamma transformation [23], and morphological techniques [24], [25]. The morphological technique is the most commonly used. However, defining the kernel size and the kernel type are the keys to obtaining a relevant result. Roopa [26] suggests a novel method to normalize and enhance a microscopic image of a thin blood smear. Normalization of green, green, and blue (GGB) is a proposed method to enhance parasites, WBC, platelets, and artifacts.

Maysanjaya et al. [27] achieved a high accuracy of 93.33% in *Plasmodium* detection. The combination of the saturation (S) channel of HSV color space and the red (R) channel of RGB color space followed by Otsu for finding the optimum threshold value was applied to segment *Plasmodium* parasites.

However, the data tested were too small in number and parasite species, with only 30 microscopy images and *Plasmodium vivax*, respectively.

Daniel et al. [28] suggested a new simple method to segment parasites. A modified double Otsu was a proposed method for automatically finding the optimum threshold value of parasites, WBC, and artifacts. The proposed method was a simple and efficient method for determining the parasite's global threshold value. The method was applied in the green component of RGB. However, there was no pre-processing except only manual crop applied. Instead, there was no evaluation reported in the segmentation stage.

Nugroho et al. [29] proposed a new scheme for *Plasmodium* detection in microscopic images of thin blood smears by combining morphology and Otsu. A median filter was applied in the pre-processing step to remove speckle noises from the image. The Otsu method was applied to find the optimum threshold value in the S-layer of HSV. The optimum threshold value was applied in thresholding the green layer of RGB color space. This study's advantage was that the tested data had noises, such as non-uniformity illumination due to microscopy light and containing artifacts. However, the data contained only 24 images.

Recent studies have proposed methods for classifying red blood cells (RBCs) as either containing parasites or not [9], [30]. However, to apply these studies, we first need to obtain the location of individual RBCs or parasite candidates. One possible starting point for obtaining parasite candidate locations is the modified double Otsu method proposed by [28]. This method has the advantage of being computationally efficient. However, the threshold value obtained using this method may not be optimal due to various factors, such as the presence of white blood cells (WBCs), low-intensity *Plasmodium*, uneven luminance, and artifacts. As a result, several parasites may be eliminated, while many RBCs may be incorrectly selected.

The present study introduces an innovative optimization algorithm for the double Otsu algorithm suggested by [28], which enables us to determine parasite threshold values in microscopic images accurately. By applying the proposed method to the PlasmoID dataset [31], which is a challenging malaria parasite dataset from Indonesia, this study demonstrates its superior performance in extracting parasite candidate locations, compared to previous approaches.

The dataset and proposed method are discussed in Section II. In Section III, the experiment results are presented. Finally, the conclusions are drawn in Section IV.

II. MATERIALS AND METHODS

A. Data Preparation

The employed data were collected in both parasitic laboratories in the Faculty of Medicine, UGM, and Eijkman Institute which was extended version of [4]. Each image has been annotated and segmented by parasitologists known as

ground truth (GT). Then, the GT was used as a reference to measure the performance of the proposed method. Data collection was carried out by capturing hundreds of thin blood smear films. The utilized data was a combination of all types in whole life stages. The image was captured by a USB digital camera (Optilab camera) with 1000x microscope magnification. The total amount of data was 468 images with 1600x1200 pixels of resolution.

The employed data presented noises, which was an advantage of this study compared to the other as aforementioned. The noises are shown in Figure 3. The frequently used data type is shown in 3(a). RBCs and parasites are easily counted and segmented. In other cases, in Figures 3(b) and 3(c), RBCs overlap with a different background color. In Figure 3(d) and 3(e), the RBCs are possible to count; however, the background color and parasite intensity are quite a difference of 3(a), respectively. Moreover, the artifacts also appear in 3(f).

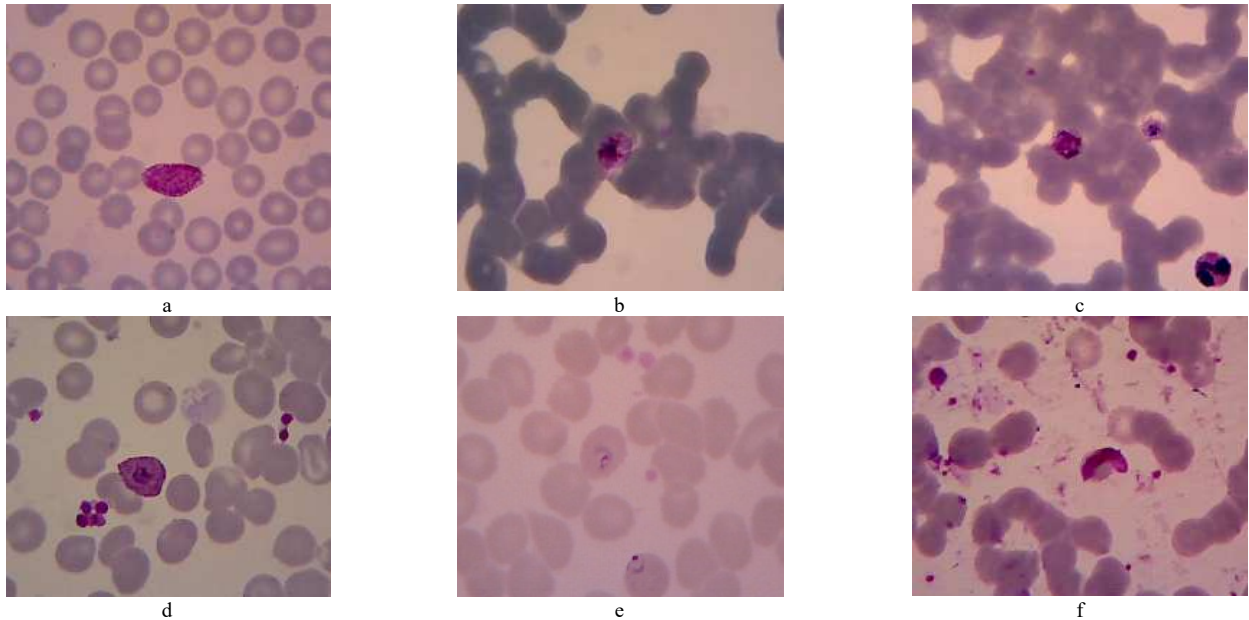


Fig. 3 Example of dataset [4] containing noises: (a) clearly image, (b)-(c) images with stacked RBC, (d)-(e) image with significant contrast difference, and (f) image with artifacts [4]

B. The Proposed Method

Extracting the parasite-infected candidate patches in our data containing artefacts and noises needs an advanced

method. A general scheme of our work is illustrated in Figure 4.

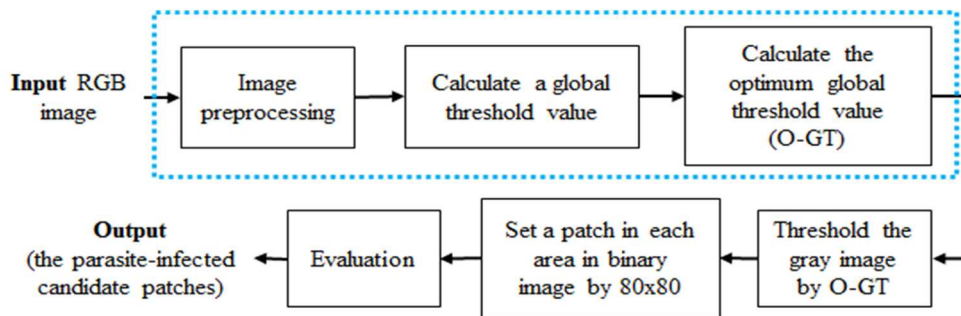


Fig. 4 Block diagram of the proposed scheme

Blue box indicates the novelty of our proposed method. The proposed method consists of three main stages. The stages were pre-processing, direct initializing the global threshold value, and finding the optimum global threshold value. The detailed process of each stage is explained as follows.

1) *Image pre-processing*: The aim of this stage was to enhance the input images. This study did not use filter techniques for eliminating a small dark area or blurring a small dark object to be unseen clear. The small dark area included parasites, WBC, and artifacts. The use of inappropriate filtering of artifacts could be a risk of losing Plasmodium malaria because the intensity values of parasites, WBC and artifact overlap. There were four steps in pre-processing, including selection of the green channel, image resizing, linear stretching, and grayscale dilation. These steps are listed in detail in Algorithm 1.

Algorithm 1. Pre-processing step

Input: RGB color image a microscopic image of a thin blood smear

Output: Image with enhanced parasite cores

1. Select the green channel (G) from RGB color space.
 2. Resize G into half of the original size.
 3. Contrast stretch G to obtain G_n using linear stretching into the range of 0-255
 4. Invert G_n to obtain G'_n using $G'_n = \max(G_n) - G_n$
 5. Apply morphological dilation with kernel 'disk' in a radius of 5 pixels.
 6. Invert back in the same way on step 4 to obtain G_1
-

The first step was to select the green channel (G) of the RGB image (original), as shown in Figure 5. The green channel was selected because the parasites would appear

brighter in an inverse image with the least noisy RGB components [32]. The second was to resize the image in order to reduce the computational time for further stage. Here, half of the resolution was reduced. Reducing the size of the utilized image was not sufficient to eliminate small parasites. In general, in microscope images with a resolution of 1600x1200 pixels, small parasites are still represented by tens of pixels. After resizing, the image resolution became 800x600.

The third was to conduct linear stretching. To unique of the scale of each image, linear stretching was applied to obtain G_n . The next step was to inverse the image to obtain G'_n . The final step was to conduct the morphological closing. The morphological operation aimed to enhance the image quality by equalizing the histogram in the dark area which represented the parasite candidates.

2) *Early determination of the global threshold value*: A simple initialization of global threshold value is intended to obtain the global threshold value of the background and objects possessing low intensity, including parasites and other artifacts. Otsu method was applied to automatically execute clustering-based image thresholding [33], or the binarization of a grayscale image. The method categorizes the pixels into two classes (foreground and background) or more classes for the modified method by calculating a threshold that minimizes intra-class intensity variance. In this malaria detection case, the parasites had a relatively different intensity from RBC and the background. However, the parasites had a much smaller size than them, as shown in Figure 6(a). It caused the Otsu method often to obtain the value threshold of RBC and background. Otsu's method modified by [28] aimed to obtain the threshold value of parasites and artifacts. Because the modified method was efficient, the method was adopted in this study for identifying the initial threshold value. The detail list of processes is shown in Algorithm 2.

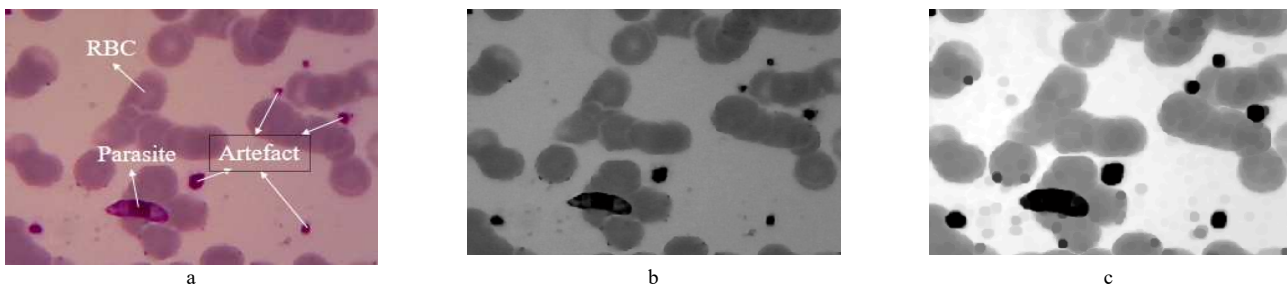


Fig. 5 An example of a microscopic image of a thin blood smear in the pre-processing stage. (a) Original image infected by Plasmodium malaria parasites with several artifacts [4], (b) green channel, and (c) the output of the pre-processing stage

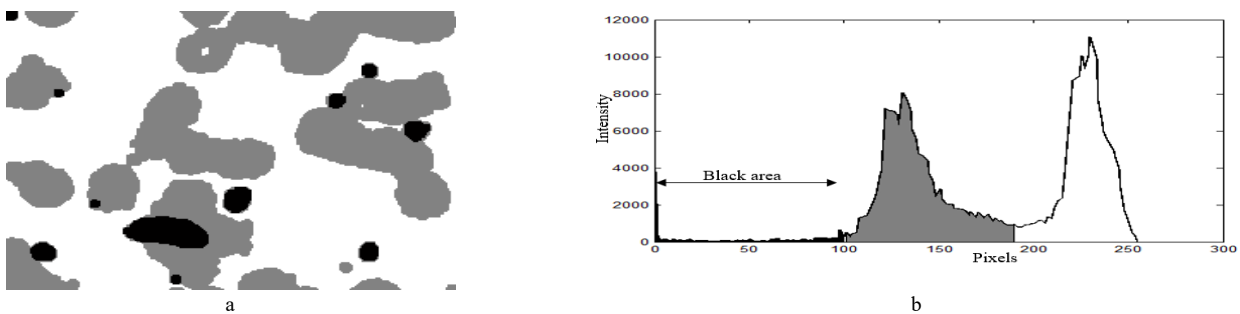


Fig. 6 Three parts are easily distinguished by the human eye including, background, RBC and Plasmodium, and several artifacts. (a) Group of intensity in a blood smear image. (b) Histogram of the image.

h_o is the histogram of the output image I_o obtained from the pre-processing stage. Otsu's method was applied to obtain the global minimum point (T_o). Here, T_o was assumed as the global threshold between RBC and background. Only the first component of T_o in h_o symbolized h_1 was used for the next step. Otsu's method was applied for a second time to obtain the second global minimum point T_1 assumed as the global threshold value of parasites. Up to this point, the global threshold was still fragile in getting all parasites on the image containing the luminance noise produced by the microscope bulb or non-homogeneous staining. Therefore, an optimized global threshold was needed.

Algorithm 2. Determination of global threshold value.

Input: Image with enhanced parasite cores

Output: New histogram with the general threshold value

1. Calculate the grayscale histogram (h_o) of the output image I_o of the pre-processing stage.
 2. Apply Otsu's method to define the global minimum point (T_o) of the histogram (h_o).
 3. Put the first elements T_o of the histogram (h_o) to obtain (h_1), $h_1 = h_o(1:T_o)$
 4. Apply the second use of the Otsu method to determine a new global minimum point (T_1), for the histogram (h_1).
-

3) *Determination of the optimum global threshold value:* This stage was the key to the novelty of this study. In the third stage, the global threshold value of parasites had been obtained. However, the optimum of the global threshold value was necessary to be extracted to detect all parasites. In Figure 6 (b), in the histogram, parasite intensity is located in the black area. Around the end of the black area is the optimum threshold value in detecting all parasites.

Algorithm 3. Determination of predicted threshold value

Input: Grayscale histogram h_1

Output: Predicted optimum global threshold values (un)

1. Calculate absolute mean and standard deviation in every three interpolations ordered of h_1 to obtain m and std_h variables, respectively.
 2. Add both variables together to obtain C to get new histogram,
 $C = m + std_h$
 3. Calculate the max reference (P) by calculating the mean of the first element T_1 of the histogram (h_1) to get mean of dark intensity, $P = \text{mean}(C[1:T_1])$
 4. Create zero variable (un) with the same size of C
 5. Put 1 in un at the location of C elements which did not have more than P
-

There were two steps to obtain the optimum global threshold value T_2 . The first is to find the predicted optimum global threshold values (un) and followed by finding the optimum global threshold value (T_2). Both steps are listed in Algorithm 3 and Algorithm 4, respectively. In Algorithm 3, mean (m) and standard deviation (std_h) were extracted of each three interpolations of h_1 . Standard deviation could be represented the stability of the histogram h_1 . Adding between std_h and m intended to remove speckle noise and to enhance the histogram. Steps 3 to 5 were to calculate the reference of the maximum number of pixels suspected that there was no parasite had more numbers than the reference. The step intended to avoid over-segmentation on RBC areas.

The output of this algorithm was the predictive threshold values that met this rule.

Algorithm 4 intended to find the optimum threshold values. The predicted threshold value values by Algorithm 3. The created algorithm purposes to avoid over-segmentation because of the lowest position of both the histogram peaks in Figure 6 was lower than P . This condition allowed for a wide space in both two predicted threshold values. Algorithm 4 was proposed to solve this case. A derivative of un' following wide detection was calculated for detecting the abnormal width. An abnormal width could be detected using the percent width of the histogram.

Algorithm 4. Determination of optimum global threshold

Input: The predicted optimum global threshold values P

Output: Optimum global threshold value (T_2)

1. Calculate un' by using 1st derivative of un
 2. Find the position of a non-zeros element of un' to obtain k
 3. Update un by using Algorithm 5
 4. Define T_2 by finding the last location of un which equals one
-

Here, 20% was determined. The optimum threshold value was obtained from the last predicted threshold values before meeting the abnormal width.

4) *Evaluation:* The focus of this study is on the extraction of parasite candidates as the initial step of a whole parasite detection method. To achieve this, we propose an optimization method for the double Otsu algorithm [28] that aims to find a general parasite threshold in microscopic images. To evaluate the performance of our proposed optimization method, we compare it with the original [28] and another previous method [29]. We assess important parameters such as the number of false positives, true positives, false negatives, sensitivity, and computational time [34].

III. RESULTS AND DISCUSSION

The robust method for detecting malaria infection in microscopic images of thin blood smears is proposed in this study. The proposed method was tested and evaluated in 468 microscopic images captured from hundreds of thin blood smears. The dataset contains 691 malaria parasites with all variants and their life stages. The previous method, [29] and [28], were also compared to show the advantages and disadvantages of the proposed method. Some parameters in the confusion matrix were involved in measuring the performance. The parameters consisted of True Positive (TP), False negative (FN), False positive (FP), and computational time. TP was the number of detected parasites correctly. FN was the number of undetected parasites. Then, FP was the number of non-parasites detected as parasites. The definition of the accurately detected parasites was determined by containing more than 50% of the body's parasite in 80 by 80 patches.

The comparison of [29] and [28] is listed in Table 1. The proposed method by [29] has the highest number of undetected parasites (FN) yet possessing the lowest FP. This effect occurs because the method is designed with many fixed parameters. Since the method was examined in the data that have artifacts and has different luminance type, the method [29] becomes not reliable. The main factor of the

unsuccessfulness of this study is the application of many morphological operations with large kernel sizes. The effect of using many morphological operations with a fixed large size is shown in Figure 7. The blue contour is a suspected parasite area determined by the system. Red contour is the ground truth. Yellow and green boxes are artifacts and detected parasites by the system, respectively.

The simple method with fast computation of 0.039s per image for finding the general threshold value was proposed by [28]. The method was designed by using the modified Otsu's to determine the global threshold value for the parasite. However, because the data used were more varied, the method's performance worsened. As reported in Table 1, [28] produces many false-positive rates with 43,678 objects and fails to detect all parasite objects, leaving 14 undetected parasite objects. Based on these results, two conditions cause [28]'s performance to be worse.

TABLE I
THE COMPARISON OF SEVERAL METHODS

Methods	TP	FN	FP	Time (s)	Sensitivity (%)
[29]	569	122	1,340	0.489	82.3
Double Otsu [28]	677	14	43,678	0.039	98
Optimized Double Otsu (Proposed)	688	3	3,555	0.073	99.6

First, when an image has black components, e.g., parasites, platelets, or white blood cells (WBC), as illustrated in Fig. 5, which has a small size indicated by a flat histogram in the low-intensity area, the [28] determines the global threshold value T_1 in the range of red blood cell intensity, as shown in Fig. 7 (b). This condition makes the number of FP significantly increase, as listed in Table 1.

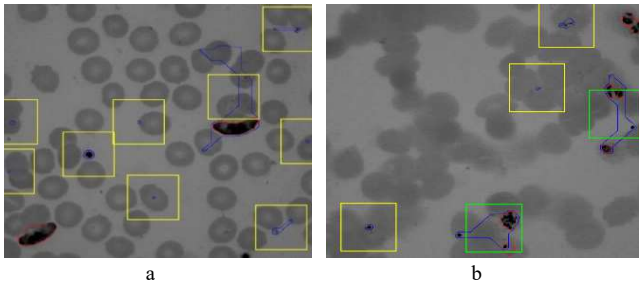


Fig. 7 Two instances of unsuccessful results of [28]

Second, when an image contains very low-intensity white blood cells (WBCs) with some parasites having a relatively high intensity, [28]'s method will determine the global threshold T_1 below the parasite intensity. Therefore, this method is difficult to detect parasites or increases the number of FN (leaving 14 parasites), as listed in Table 1. However, when an image is executed without these conditions, and the

parasites size is relatively large, implementing [28] is still considered. Considering these two conditions, our method is proposed to decrease the number of false negative rate and false positive rate.

There are two steps added in modifying [28] as novelties of this research to achieve better performance in malaria detection. First, to reduce FP, a pre-processing step is added. This scheme was designed by applying morphological dilation in greyscale for homogenizing the surface. Second, to reduce FN, an optimization of the original is introduced.

Figure 8 shows some results in segmenting parasite using different methods to generate a global threshold value on a microscopic thin blood smear image. Figure 8(a) is an example of the previous method [28] in extracting the parasite patch candidates in our dataset. Because the image contains a heavy clumped RBC, the second global threshold value (T_1) aiming to segment the parasites lies on the RBC's intensity rank, as shown in Figure 8(b). Consequently, many RBC parts are also segmented, as shown in Figure 8(a).

After we add the pre-processing step, the second global threshold value (T_1) is successfully laid on the parasite's intensity range, as shown in Figure 8(d). It can significantly compress the number of FPs. However, the laid T_1 is too backward, middle on the parasite's intensity range. That position has a chance to miss a bright parasite. The missed parasite is shown in Figure 8(c).

To overcome this issue, we proposed an optimized method to rest the global threshold value on the border parasite's intensity range (T_2), as shown in Figure 8(e). Several points suspected as the optimal locations of T_1 (C) were obtained by using the optimization method. The T_2 laid on the last of C , which was the optimum border of the back area, as shown in Figure 6. Our method was successful in reducing both of the limitations, FN and FP. The optimized [28] achieves better performance than the [28] with only three FNs are remained and more than half of the total FPs are successfully reduced, as listed on Table 1.

The proposed method obtains better results than the original [28] by optimizing and adding a pre-processing into the [28]'s method. However, referring to Table 1, there are three undetected parasites by the proposed method or 99.6% for the sensitivity, as shown in Table 2. It is a disadvantage of using the pre-processing scheme. Figure 9 shows an example of a parasite that is not successfully detected. Figure 9(a) is the original image comprising three parasites. Two parasites have different high intensities; the last has a similar intensity with RBCs. The miss detection of a parasite is because the pre-processing scheme enhances the surface of the two parasite cores. However, the last parasite possessing similar intensity with RBC is harder to find the optimum threshold. Extracting the parasite-infected candidate patches was a study's scope, whereas image classification methods can reduce the number of FPs in further research.

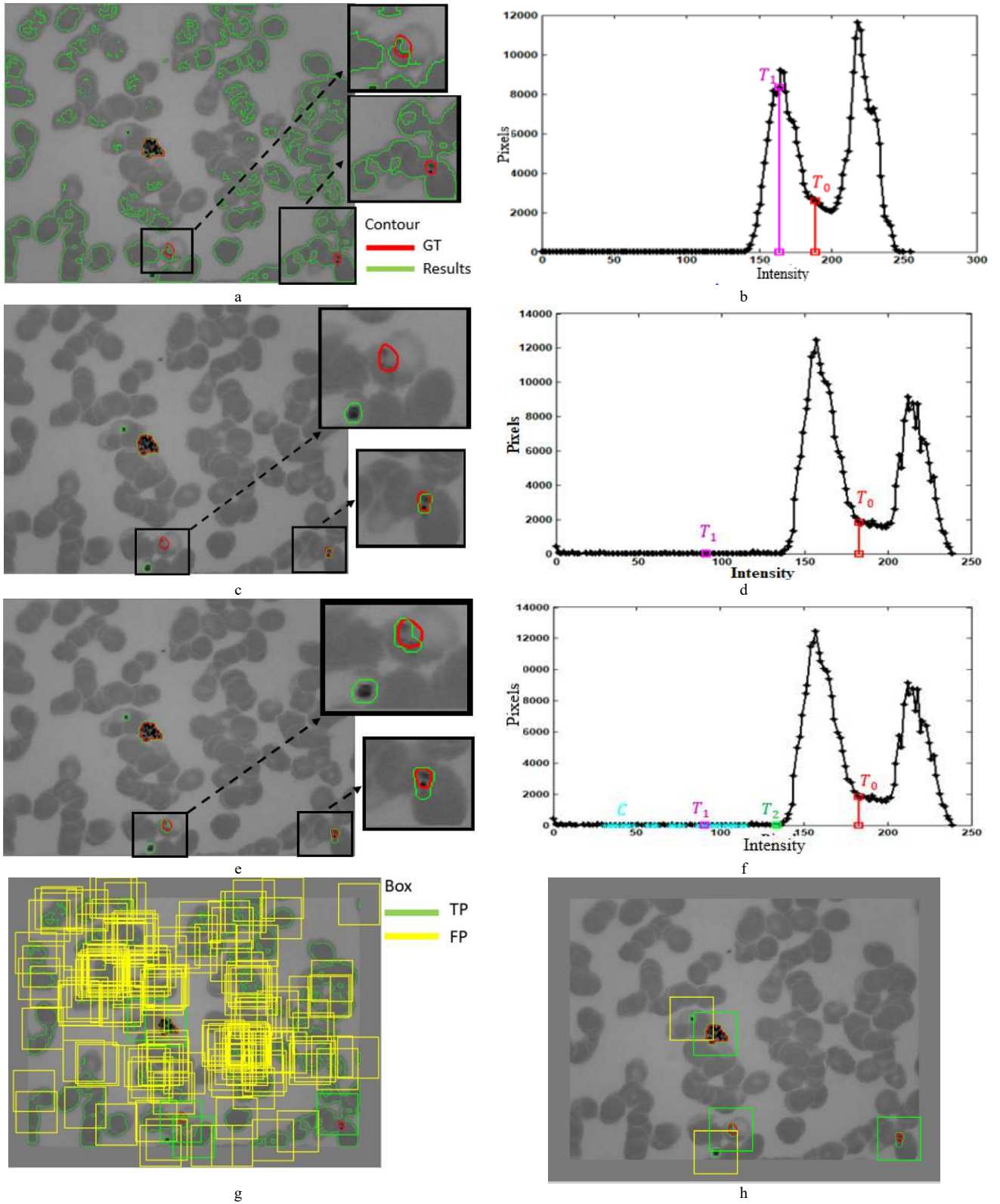


Fig. 8 The comparison methods in detecting parasites using: (a) the original of [28] with (b) its corresponding histogram, (c) [28]'s modification by adding pre-processing with (d) its corresponding histogram, (e) the proposed method with (f) its corresponding histogram and (g) the results in patch detection of the original [28] and (h) the proposed method, respectively

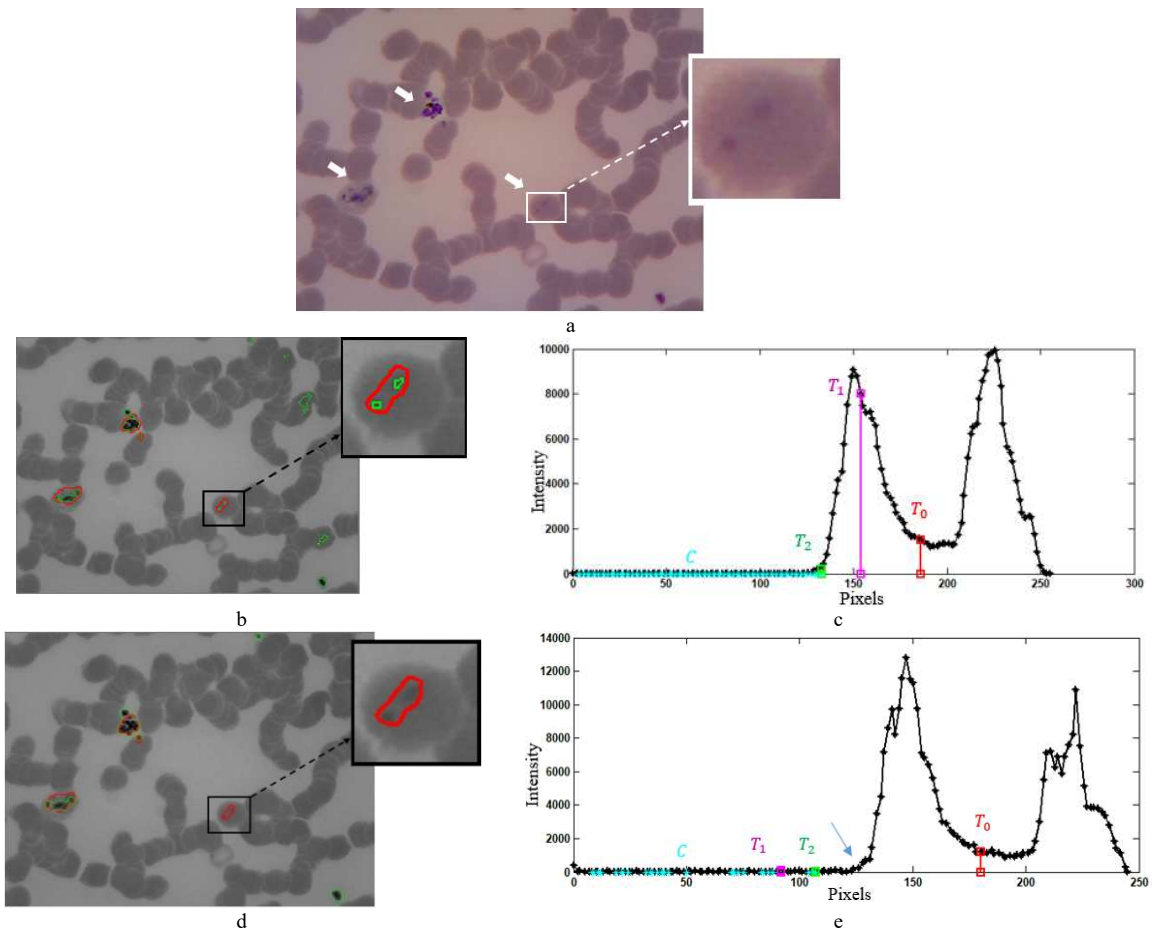


Fig. 9 Missing detection of a parasite in (a) an image from dataset [4] is treated by (b) [28]+prep with (c) its corresponding histogram and (d) the proposed method with (e) its corresponding histogram.

IV. CONCLUSION

This paper proposes a method for finding the optimum global threshold value for early malaria detection, extracting the parasite-infected candidate patches in microscopic thin blood smear images. This early step is very important since it was used as an initial step in the parasite candidate detection process. Our proposed method was performed on the data consisting of 468 thin blood smear images containing 691 malaria parasites. The proposed method achieves the highest sensitivity of 99.6% and the lowest number of FN (false negative) in detecting the parasite-infected candidate patches among the compared methods.

ACKNOWLEDGMENT

The acknowledge the Department of Parasitology, Faculty of Medicine, Public Health and Nursing, Universitas Gadjah Mada, and Eijkman Institute for Molecular Biology for providing the database in this research and also to The Department of Electrical and Information Engineering, UGM for supporting the fund in this research.

REFERENCES

- [1] Z. Jan, A. Khan, M. Sajjad, K. Muhammad, S. Rho, and I. Mehmood, "A review on automated diagnosis of malaria parasite in microscopic blood smears images," *Multimedia Tools and Applications*, vol. 77, no. 8, pp. 9801–9826, Mar. 2017, doi: 10.1007/s11042-017-4495-2.
- [2] "WHO | World malaria report 2018," *WHO*, 2018.
- [3] Ministry of Health of the Republic of Indonesia, "Eliminasi Malaria Indonesia."
- [4] H. A. Nugroho et al., "Multithresholding Approach for Segmenting Plasmodium Parasites," 2019 11th International Conference on Information Technology and Electrical Engineering (ICITEE), Oct. 2019, doi: 10.1109/icitee.2019.8929995.
- [5] J. Frean, "Microscopic determination of malaria parasite load: role of image analysis," *Microsc. Sci. Technol. Appl. Educ.*, pp. 862–866, 2010.
- [6] J. A. Quinn, A. Andama, I. Munabi, and F. N. Kiwanuka, "Automated Blood Smear Analysis for Mobile Malaria Diagnosis," *Mob. Point-of-Care Monit. Diagnostic Device Des.*, vol. 31, pp. 115–132, 2014.
- [7] M. L. Wilson, "Malaria Rapid Diagnostic Tests," *Clinical Infectious Diseases*, vol. 54, no. 11, pp. 1637–1641, May 2012, doi:10.1093/cid/cis228.
- [8] M. M. Kettelhut, "External quality assessment schemes raise standards: evidence from the UKNEQAS parasitology subschemes," *Journal of Clinical Pathology*, vol. 56, no. 12, pp. 927–932, Dec. 2003, doi: 10.1136/jcp.56.12.927.
- [9] F. B. Tek, A. G. Dempster, and I. Kale, "Computer vision for microscopy diagnosis of malaria," *Malaria Journal*, vol. 8, no. 1, Jul. 2009, doi: 10.1186/1475-2875-8-153.
- [10] R. E. Coleman et al., "Comparison of field and expert laboratory microscopy for active surveillance for asymptomatic Plasmodium falciparum and Plasmodium vivax in western Thailand," *The American Journal of Tropical Medicine and Hygiene*, vol. 67, no. 2, pp. 141–144, Aug. 2002, doi: 10.4269/ajtmh.2002.67.141.
- [11] I. Bates, V. Bekoe, and A. Asamoah-Adu, *Malaria Journal*, vol. 3, no. 1, p. 38, 2004, doi: 10.1186/1475-2875-3-38.
- [12] K. Mitiku, G. Mengistu, and B. Gelaw, "The reliability of blood film examination for malaria at the peripheral health unit," *Ethiop. J. Heal. Dev.*, vol. 17, no. 3, pp. 197–204, 2003.
- [13] World Health Organization, "Basic malaria microscopy – Part I: Learner's guide," Second ed., 2010.

- [14] A. Moody, "Rapid Diagnostic Tests for Malaria Parasites," *Clinical Microbiology Reviews*, vol. 15, no. 1, pp. 66–78, Jan. 2002, doi:10.1128/cmr.15.1.66-78.2002.
- [15] M. Poostchi, K. Silamut, R. J. Maude, S. Jaeger, and G. Thoma, "Image analysis and machine learning for detecting malaria," *Translational Research*, vol. 194, pp. 36–55, Apr. 2018, doi:10.1016/j.trsl.2017.12.004.
- [16] B. R. Mirdha, J. C. Samantaray, and B. Mishra, "Laboratory diagnosis of malaria," *Journal of Clinical Pathology*, vol. 50, no. 4, pp. 356–356, Apr. 1997, doi: 10.1136/jcp.50.4.356-a.
- [17] A. Ajala, Funmilola. A, F. Fenwa, Olusayo. D, A. Aku, and Micheal. A., "Comparative Analysis of different types of Malaria Diseases using First Order Features," *International Journal of Applied Information Systems*, vol. 8, no. 3, pp. 20–26, Feb. 2015, doi:10.5120/ijais15-451297.
- [18] H. Tulsani and S. Saxena, "Segmentation using Morphological Watershed Transformation for Counting Blood Cells," *Int. J. Comput. Appl. Inf. Technol.*, vol. 2, p. 28.
- [19] D. Yang et al., "A portable image-based cytometer for rapid malaria detection and quantification," *PLOS ONE*, vol. 12, no. 6, p. e0179161, Jun. 2017, doi: 10.1371/journal.pone.0179161.
- [20] D. K. Das, M. Ghosh, M. Pal, A. K. Maiti, and C. Chakraborty, "Machine learning approach for automated screening of malaria parasite using light microscopic images," *Micron*, vol. 45, pp. 97–106, Feb. 2013, doi: 10.1016/j.micron.2012.11.002.
- [21] D. K. Das, C. Chakraborty, B. Mitra, A. K. Maiti, and A. K. Ray, "Quantitative microscopy approach for shape - based erythrocytes characterization in anaemia," *Journal of Microscopy*, vol. 249, no. 2, pp. 136 – 149, Dec. 2012, doi: 10.1111/jmi.12002.
- [22] C. Ma, P. Harrison, L. Wang, and R. L. Coppel, "Automated estimation of parasitaemia of Plasmodium yoelii-infected mice by digital image analysis of Giemsa-stained thin blood smears," *Malaria Journal*, vol. 9, no. 1, Dec. 2010, doi: 10.1186/1475-2875-9-348.
- [23] A. Skandarajah, C. D. Reber, N. A. Switz, and D. A. Fletcher, "Quantitative Imaging with a Mobile Phone Microscope," *PLoS ONE*, vol. 9, no. 5, p. e96906, May 2014, doi:10.1371/journal.pone.0096906.
- [24] S. Kaewkamnerd, C. Uthapibull, A. Intarapanich, M. Pannarut, S. Chaotheing, and S. Tongsim, "An automatic device for detection and classification of malaria parasite species in thick blood film," *BMC Bioinformatics*, vol. 13, no. S17, Dec. 2012, doi:10.1186/1471-2105-13-s17-s18.
- [25] M. Imroze Khan, B. Acharya, B. Kumar Singh, and J. Soni, "Content Based Image Retrieval Approaches for Detection of Malarial Parasite in Blood Images," *Int. J. Biometrics Bioinforma.*, vol. 5, no. 2, pp. 97–110, 2011.
- [26] R. B. Hegde, K. Prasad, H. Hebbar, and B. M. K. Singh, "Development of a robust algorithm for detection of nuclei of white blood cells in peripheral blood smear images," *Multimedia Tools and Applications*, vol. 78, no. 13, pp. 17879–17898, Jan. 2019, doi:10.1007/s11042-018-7107-x.
- [27] I. Md. D. Maysanjaya, H. A. Nugroho, N. A. Setiawan, and E. E. H. Murhandarwati, "Segmentation of Plasmodium vivax phase on digital microscopic images of thin blood films using colour channel combination and Otsu method," *AIP Conference Proceedings*, 2016, doi: 10.1063/1.4958595.
- [28] D. M. Memeu, K. A. Kaduki, A. C. K. Mjomba, N. S. Muriuki, and L. Gitonga, "Detection of plasmodium parasites from images of thin blood smears," *Open Journal of Clinical Diagnostics*, vol. 03, no. 04, pp. 183–194, 2013, doi: 10.4236/ojcd.2013.34034.
- [29] H. A. Nugroho, W. A. Saputra, A. E. Permanasari, and E. E. H. Murhandarwati, "Automated determination of Plasmodium region of interest on thin blood smear images," *2017 International Seminar on Intelligent Technology and Its Applications (ISITIA)*, Aug. 2017, doi:10.1109/isitia.2017.8124108.
- [30] S. Rajaraman et al., "Pre-trained convolutional neural networks as feature extractors toward improved malaria parasite detection in thin blood smear images," *PeerJ*, vol. 6, p. e4568, Apr. 2018, doi:10.7717/peerj.4568.
- [31] H. A. Nugroho, R. Nurfauzi, E. E. H. Murhandarwati, and P. Purwono, "PlasmoID: A dataset for Indonesian malaria parasite detection and segmentation in thin blood smear." 2022.
- [32] N. E. Ross, C. J. Pritchard, D. M. Rubin, and A. G. Dusé, "Automated image processing method for the diagnosis and classification of malaria on thin blood smears," *Medical & Biological Engineering & Computing*, vol. 44, no. 5, pp. 427–436, Apr. 2006, doi: 10.1007/s11517-006-0044-2.
- [33] B. Sankur, "Survey over image thresholding techniques and quantitative performance evaluation," *Journal of Electronic Imaging*, vol. 13, no. 1, p. 146, Jan. 2004, doi: 10.1117/1.1631315.
- [34] B. Durakovic, "Design of experiments application, concepts, examples: State of the art," *Periodicals of Engineering and Natural Sciences (PEN)*, vol. 5, no. 3, Dec. 2017, doi: 10.21533/pen.v5i3.145.